

Polyisobutene–poly(methylmethacrylate) interpenetrating polymer networks: synthesis and characterization

Cédric Vancaeyzeele^a, Odile Fichet^a, Sylvie Boileau^b, Dominique Teyssié^{a,*}

^a*Laboratoire de Physico-chimie des Polymères et des Interfaces (LPPI), Université de Cergy-Pontoise, 5, mail Gay-Lussac, Neuville-sur-Oise, 95031 Cergy-Pontoise Cedex, France*

^b*Laboratoire de Recherche sur les Polymères, UMR 7581 CNRS, 2, rue H.Dunant, 94320 Thiais, France*

Received 11 March 2005; received in revised form 20 May 2005; accepted 23 May 2005

Available online 16 June 2005

Abstract

Interpenetrating polymer networks (IPNs) combining polyisobutene (PIB) and poly(methyl methacrylate) (PMMA) networks were prepared using a *in situ* strategy. PIB networks were formed by isocyanate–alcohol addition between the hydroxyl end groups of telechelic dihydroxy-polyisobutene and an isocyanate cross-linker, catalyzed by dibutyltindilaurate (DBTDL). PMMA networks were obtained from free-radical co-polymerization of methyl methacrylate (MMA) with ethylene glycol bismethacrylate (EGDM) in the presence of dicyclohexyl peroxydicarbonate (DCPD) as the initiator. The synthesis of each network during the IPN formation was followed by FTIR spectroscopy. The highest degree of interpenetration is obtained by forming the PIB network first. The corresponding transparent IPNs exhibit two mechanical relaxation temperatures as determined by Dynamic mechanical thermal analysis (DMTA), corresponding to those of PMMA and PIB enriched phases. Mechanical properties of PIB networks are tremendously improved by the presence of PMMA network in such IPN architecture.

© 2005 Elsevier Ltd. All rights reserved.

Keywords: Interpenetrating polymer networks; α,ω -Dihydroxy polyisobutene; Poly(methyl methacrylate)

1. Introduction

Polyisobutene rubbers are well-known to have special properties such as resistance to gas and moisture permeation or penetration, high elasticity and flexibility at extreme temperatures particularly in the low range. Their glass transition temperatures can be as low as $-76\text{ }^{\circ}\text{C}$. Polyisobutenes have also excellent resistance to weathering and ultraviolet light [1]. Nevertheless, polyisobutene materials exhibit poor mechanical properties due to creeping, low resistance to impact and penetration. These materials are not resistant to organic solvents (benzene, toluene or petroleum ethers) and to solvent containing materials such as lacquers, fats and oils.

In order to enlarge the field of potential applications of

polyisobutenes [2], the syntheses of polyisobutene combinations with various polymers exhibiting better mechanical properties have been investigated.

Combinations of PIB with thermoplastics for instance might help to partly at least overcome the elastomer's weaknesses, the challenge being not to impair their low gas permeability. Such combinations must be stable over time and can be achieved out by blending or copolymer elaboration. Another possibility to obtain a thermoplastic reinforced elastomer is to combine both polymers into an interpenetrating polymer network (IPN) architecture, which is most generally defined as a combination of two polymer networks synthesized in juxtaposition. The entanglement of two cross-linked polymers leads to forced miscibility compared with usual blends and the resulting materials exhibit a good dimensional stability. These types of polymer associations most often lead to materials with better mechanical properties, increased resistance to degradation and a possibly synergistic combination of the properties of their components. IPNs can be prepared through different synthetic routes described in the literature among which the *in situ* technique usually proves to be the most convenient

* Corresponding author. Tel.: +33 1 34 25 70 50; fax: +33 1 34 25 70 70.

E-mail address: dominique.teyssié@chim.u-cergy.fr (D. Teyssié).

technique [3,4]. In this in situ polymerization strategy, all reactants are mixed together and the reactions leading to the formation of the two networks can be started at the same time leading either to the simultaneous formation of the networks or to a more or less sequential one depending on the experimental conditions. Hence, if this method is to be used, the reaction mechanisms leading to the two network partners must preferably be of different nature, otherwise a single copolymer network is formed.

To our knowledge, the synthesis of IPNs containing a PIB network as one of the partners has not been reported yet in the literature. Indeed, Kennedy et al. have reported the synthesis and the characterizations of PIB/poly(dimethylsiloxane) bicomponent networks [5–7], but in this material, PDMS chains are cross-linked through allyl-trifunctional polyisobutene via a hydrosilylation reaction. Bicomponent new nanostructured co-networks of poly(ethyl acrylate)-linked-polyisobutene were synthesized from copolymerization of α,ω -dimethacrylic PIB and ethylacrylate on one hand [8] and poly(ethyleneoxide)-linked-polyisobutene co-networks were prepared from condensation of hydroxy-telechelic three-arm star PIB with isocyanate telechelic polyethyleneglycol on the other hand [9]. Finally, a new class of amphiphilic polyelectrolyte co-networks composed of hydrophobic polyisobutene and hydrophilic poly(methacrylic acid) segments was prepared in a broad range of composition [10]. In all above cases, the materials are co-networks.

On the other hand, as far as thermoplastic/elastomer combinations are concerned, polymethylmethacrylate (PMMA) has been associated with polybutadiene [11,12], polydimethylsiloxane [13–18] and polymethylphenylsiloxane [19] into IPN architecture. Those materials are all biphasic and each of them shows two glass transition temperatures corresponding to enriched phases in one or the other partner. The thermomechanical properties of the elastomeric partner in each case have been improved as expected. As far as PIB/PMMA combinations are concerned, a material composed of dispersed and covalently bound PIB to a PMMA matrix has been synthesized for cement bone application. This material resistance and flexibility depend on each polymer weight proportion [20].

Similarly the aim of this work is to improve the mechanical properties of polyisobutene by combining it into an IPN architecture with PMMA. This involves a in situ strategy in which all components are first mixed together and the networks are then formed more or less simultaneously as it will be shown, according to different reaction mechanisms. The conversion as a function of time of reactive functions involved in the synthesis of each network during the IPN formation has been investigated by near FTIR spectroscopy. In order to examine the extent of network interpenetration, thermomechanical properties of the resulting materials have been studied by dynamic mechanical thermal analysis (DMTA) and they have been characterized by AFM microscopy.

2. Experimental part

2.1. Materials

α,ω -Dihydroxypolyisobutene ($M_{n\text{ SEC}}=4200\text{ g mol}^{-1}$, $I_p=1.2$ in THF, $M_{\text{NMR}}=5400\text{ g mol}^{-1}$ in CDCl_3) was kindly provided by BASF. Dibutyltindilaurate (DBTDL) (Aldrich), ethylene glycol bismethacrylate (EGDM) (Aldrich), benzoin methyl ether (Acros) and Desmodur N3300[®] (Bayer) (NCO content by weight: $21.8\% \pm 0.3\%$ according to the supplier) were used as received. This last compound is described as an isocyanurate mixture resulting from the condensation of three to several hexamethylene diisocyanate molecules and mainly composed of mono-, di- and tri-isocyanurates with a global functionality higher than 2 [21]. Thus mere ‘tri(6-isocyanatohexyl)isocyanurate’ is not a proper description and the compound is referred to as isocyanate cross-linker or cross-linking agent. Dicyclohexyl peroxydicarbonate (DCPD, group Arnaud) was dried under vacuum before use. Methyl methacrylate (MMA, Acros) and toluene (Prolabo) were distilled before use. Dichloromethane (CH_2Cl_2 , Carlo Erba) was used as received.

2.2. Synthesis

2.2.1. PIB single networks

α,ω -Dihydroxypolyisobutene (1 g, 4.5×10^{-4} OH mol equiv.) was mixed with Desmodur[®] N3300 (0.13 g, 6.8×10^{-4} NCO mol, $[\text{NCO}]/[\text{OH}]=1.5$) in 2 mL toluene to which the catalyst, DBTDL (3 μL , 5.9×10^{-6} mol, $[\text{DBTDL}]/[\text{OH}]=0.013$) was added. The mixture was poured under argon into a mould made from two glass plates clamped together and sealed with a 0.5 mm thick Teflon[®] gasket. The mould was heated in an oven at 40 °C for 6 h and annealed for 1 h at 80 °C. A transparent film is obtained once the toluene is taken off under vacuum.

2.2.2. PMMA single networks

MMA (1 g, 1.0×10^{-2} mol) was mixed with 30 mg EGDM (1.5×10^{-4} mol, 3% by weight with respect to MMA) and 5 mg DCPD free radical initiator (1.7×10^{-5} mol, 0.5% by weight with respect to MMA). The mixture was poured under argon into a mould made from two glass plates clamped together and sealed with a 0.5 mm thick Teflon[®] gasket. The mould was heated in an oven at 40 °C for 6 h and then at 80 °C for 1 h. A rigid transparent film is obtained.

2.2.3. PIB/PMMA IPNs

For the PIB/PMMA (50/50) IPN, 1 g α,ω -dihydroxypolyisobutene (4.5×10^{-4} OH mol equiv.) was mixed with 1 g MMA (1.0×10^{-2} mol) and 30 mg EGDM (1.5×10^{-4} mol, 3% by weight with respect to MMA) in 0.2 mL toluene under argon. Then 5 mg DCPD (1.7×10^{-5} mol, 0.5% by weight with respect to MMA), 0.13 g Desmodur[®] N3300 ($[\text{NCO}]/[\text{OH}]=1.5$) and 3 μL DBTDL ($[\text{DBTDL}]/[\text{OH}]=$

0.013) were added. The solution was degassed and then poured under argon into a mould, as described previously. The mould was heated in an oven at 40 °C for 6 h, and then at 80 °C for 1 h.

IPNs with different PMMA contents ranging from 30 to 80% by weight were synthesized keeping the same proportions between monomer, cross-linker and catalyst or initiator for each network. All investigated PIB/PMMA compositions are reported in weight by weight ratio. Thus, an IPN obtained from a mixture of 0.70 g α,ω -dihydroxypolyisobutene and 0.30 g PMMA will be noted PIB/PMMA (70/30) IPN.

2.3. Analytical techniques

2.3.1. Extractible products

In order to estimate the amount of uncross-linked starting material in the final product and thus the extent of network formation, single networks and IPNs were extracted in a Soxhlet with dichloromethane for 72 h. After extraction, the sample was dried under vacuum and then weighed. The extracted content (EC) is given as a weight percentage:

$$EC(\%) = \frac{(W_0 - W_E)}{W_0} \times 100$$

where W_0 and W_E are the weights of samples before and after extraction, respectively.

2.3.2. FTIR spectroscopy

In the case of single networks and PIB/PMMA IPNs, the rates of the network formation were followed in the bulk, in real time, in the near and middle infrared (NIR and MIR) regions (7500–1800 cm^{-1}). The PMMA network formation as well as that of the urethane bonds were followed by monitoring the disappearance of the H–C=C overtone absorption bands at 6167 cm^{-1} [22] and that of the isocyanate function at 2270 cm^{-1} [23], respectively, as described previously [24]. A given peak area is directly proportional to the reagent concentration (the Beer–Lambert law has been verified), thus the conversion–time profile can be easily derived from the spectra recorded as a function of time. The conversion of reactive bonds can be calculated as $p = 1 - (A_t/A_0)$ from the absorbance values, where the symbols have the usual meaning and the subscripts 0 and t denote reaction times.

IPNs were directly synthesized in the IR cell which is made from two calcium fluoride plates separated by a 250 μm thick Teflon[®] gasket. Indeed in the 100–300 μm thickness range the measured absorbance follows the Beer–Lambert law, which is not the case for the 500–1000 μm thick samples used in the DMTA characterizations. The IR cell was inserted in an electrical heating jacket with an automatic temperature controller (Graseby Specac). The temperature of the cell holder was constant within ± 1 °C of the set temperature. The infrared spectra were recorded with

a Bruker spectrometer (Equinox 55) in the range 7000–1800 cm^{-1} by averaging 10 consecutive scans with a resolution of 4 cm^{-1} . Scan accumulations were repeated every 5 min during the kinetic measurements.

2.3.3. Atomic force microscopy

Atomic force microscopy (AFM) apparatus is composed of a Dimension 3100 scanning probe microscope and a NanoScope[®] IIIa from VEECO. The scanning window can vary from 100 μm down to a few nanometers. The probe tip frequency resonance is $f_0 = 250$ kHz.

2.3.4. Dynamic mechanical thermal analysis

Dynamic mechanical thermal analysis (DMTA) measurements were carried out on film samples with a Q800 apparatus (TA Instruments) operating in tension mode. Experiments were performed at a 1 Hz frequency and a heating rate of 3 °C min^{-1} from –100 to 200 °C. Typical dimensions of the samples were 30 \times 8 \times 0.5 mm^3 . The set up provides the storage and loss modulus (E' and E'') and the damping parameter or loss factor ($\tan \delta$). All storage modulus values were normalized at 3 GPa at –100 °C when the materials are in a glassy state, in order to compare their relative evolution with increasing temperature.

3. Results and discussion

Before combining PIB and PMMA into an IPN architecture, single networks have been synthesized and characterized in order to establish the most convenient experimental conditions.

3.1. Individual networks

The PIB single network is synthesized via an alcohol/isocyanate condensation reaction between α,ω -dihydroxypolyisobutene and isocyanate cross-linker, catalyzed by DBTDL. Due to the very high viscosity of the α,ω -dihydroxypolyisobutene, it appeared unavoidable to add a minimum amount of toluene as a solvent, in order to ensure a homogeneous distribution of cross-linking agent and catalyst. After thermal cure, and then evaporation of the remaining toluene under vacuum an insoluble transparent material which contains a very low amount of extractible products (about 1%) as found by a Soxhlet extraction with CH_2Cl_2 , is obtained.

The storage modulus (E') and the loss tangent ($\tan \delta$) of this single PIB network are reported in Fig. 1. Schematically, three temperature domains are observed. From –100 to –70 °C, the polymer is in the glassy state: the storage modulus E' is almost constant at 3 GPa. The response of the network is mainly elastic. Above –70 °C, a strong decay of elastic part of the modulus E' is observed while $\tan \delta$ vs. temperature curve presents a maximum at –30 °C ($\tan \delta = 1.28$). The α -relaxation is quite broad and is composed of a

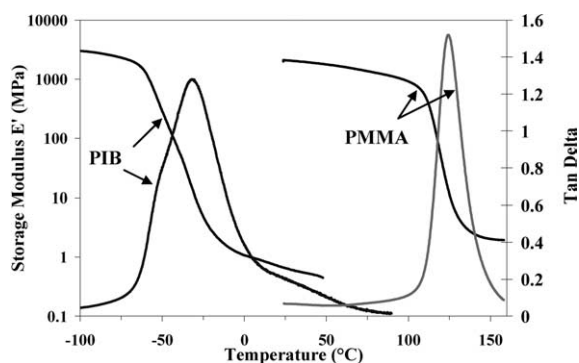


Fig. 1. PIB and PMMA single network storage modulus E' (black) and $\tan \delta$ (grey) variations vs. temperature.

peak centered at $-30\text{ }^{\circ}\text{C}$, corresponding to the T_{α} of PIB and a low temperature shoulder ($-50\text{ }^{\circ}\text{C}$) which has been observed in other PIB based materials [25,26]. These two mechanical relaxation temperatures have been associated to the PIB end local rotational chain motion ($T_{\alpha} = -50\text{ }^{\circ}\text{C}$) and to the PIB cooperative backbone motion ($T_{\alpha} = -30\text{ }^{\circ}\text{C}$) [27–29]. The elastic part of the modulus E' reaches a plateau (rubbery modulus) at 0.7 MPa at temperatures higher than $0\text{ }^{\circ}\text{C}$.

The PMMA network is formed by free-radical copolymerization of MMA with EGDM (3% by weight with respect to MMA) as the cross-linker, initiated by DCPD (0.5% by weight with respect to MMA). A rigid transparent material is obtained with a very low amount of extracted products ($<1\%$) as shown by a Soxhlet extraction with CH_2Cl_2 .

Thermomechanical properties of this single PMMA network are reported in Fig. 1. Below $110\text{ }^{\circ}\text{C}$, the storage modulus is almost constant at 3 GPa. Above $110\text{ }^{\circ}\text{C}$, it decreases rapidly down to a rubbery plateau value at 3 MPa. The sharp decrease of E' and the $\tan \delta$ maximum value ($\tan \delta = 1.50$) at $132\text{ }^{\circ}\text{C}$ are associated to the mechanical relaxation of PMMA.

3.2. IPNs

All the IPNs have been synthesized according to an in situ strategy, i.e. all the reagents are mixed together: monomers, cross-linkers, initiator and catalyst form a clear solution in toluene (0.1 mL/g of reaction mixture). PMMA networks are prepared by free-radical polymerization of MMA with EGDM as the cross-linker and DCPD as the initiator. The PIB cross-linking arises through the formation of urethane bonds between OH end groups of PIB and the Desmodur N3300[®] isocyanate cross-linker. Toluene is also used as a solvent in this case because PIB is not soluble in MMA.

3.2.1. Respective rates of PIB and PMMA network formation in the IPN

The respective rates of PIB and PMMA network

formation during the in situ IPN synthesis are monitored by FTIR spectroscopy in order to understand their mutual influence on the structure of the resulting three-dimensional interpenetrating network. Indeed the final network interpenetration degree is highly dependent upon the nature of the particular polymer pair which is considered and their relative order of formation. The best result is sometimes obtained through simultaneous formation of the two networks and sometimes through sequential formation, i.e. one after the other [30,31]. Simultaneous and sequential in situ strategies were thus studied in order to examine the resulting degree of interpenetration of the networks obtained in both cases.

The MMA/EGDM co-polymerization and network formation are followed by near-IR spectroscopy, by monitoring the disappearance of the absorption band of the methacrylate C–H bond at 6167 cm^{-1} [22]. The PIB network formation is followed by monitoring the disappearance vs. time of the absorption band of isocyanate groups at 2270 cm^{-1} [32,33]. The disappearance of these two absorption bands as a function of time is directly related to the reactive function conversions vs. time and thus the network conversion degree.

In a first series of experiments, the synthesis temperature is set at $40\text{ }^{\circ}\text{C}$ for 6 h since the DCPD decomposes with a convenient rate at this temperature ($k_d = 1.34 \times 10^{-5}\text{ s}^{-1}$, $t_{1/2} = 14.3\text{ h}$ [34]). On the other hand, $40\text{ }^{\circ}\text{C}$ is also a convenient temperature for the formation of the PIB network through isocyanate cross-linking agent since this compound can lead to side reactions such as biuret, allophanate and isocyanurate... formation which occur at temperatures as low as $70\text{ }^{\circ}\text{C}$ [35]. Thus, in these conditions, isocyanate functions only react with hydroxyl PIB end groups as checked by FTIR measurements. In order to determine the PIB hydroxyl group conversion during the cross-linking, it must be assumed here that each NCO group which disappears reacts with only PIB OH group (although some uncertainty remains whether a NCO group can be destroyed by contaminating water for instance). The $[\text{NCO}]/[\text{OH}]$ most efficient molar ratio was experimentally found to be equal to 1.5 in this study. Indeed, this leads to complete cross-linking of all the end chain OH groups of PIB within a reasonable length of time. This NCO excess requirement probably arises both from the high viscosity and low mobility of the PIB oligomer and the cross-linker.

A PIB/PMMA (30/70) weight proportion was chosen for the FTIR monitoring of the network formation with three different radical initiator proportions 0.1, 0.5 or 1% DCPD by weight with respect to MMA. The aim of varying the DCPD proportion was to slow down or to accelerate the PMMA network formation compared with that of the PIB one. The hydroxyl and methacrylate function conversions witnessing the formation of the two networks in the three cases are reported in Fig. 2.

With 0.1% DCPD by weight with respect to MMA (Fig. 2(a)), the conversion of the PIB network reached 60%

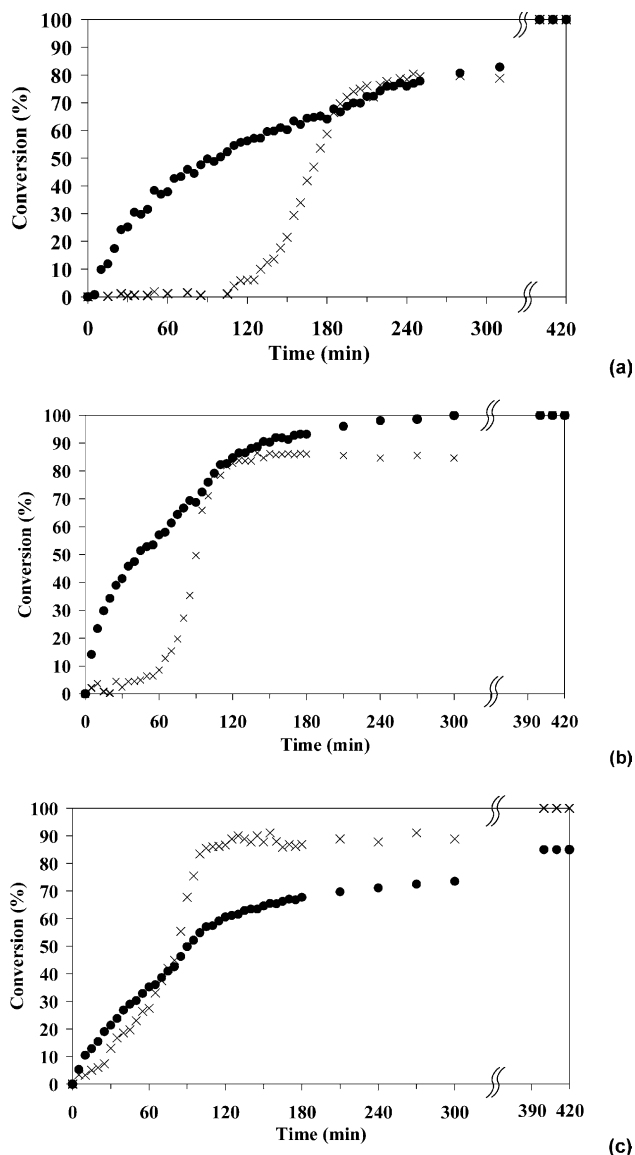


Fig. 2. Methacrylate (X) and hydroxyl (●) function conversion in PIB/PMMA (30/70) IPNs with (a) 0.1%, (b) 0.5% or (c) 1% DCPD by weight with respect to MMA. [DBTDL]/[OH]=0.013, [NCO]/[OH]=1.5, EGDM: 3% by weight with respect to MMA. $T=40^{\circ}\text{C}$.

at the time when the PMMA network formation starts, i.e. 2 h after the beginning of the reaction. This inhibition period probably corresponds to the destruction of the low DCPD radical amount by residual oxygen traces present in the reaction mixture. Under those experimental conditions, both conversion curves reach a plateau at around 80% after 4 h. After 6 h at 40°C , the material is then annealed for 1 h at 80°C in order to complete reactive function conversion. The final material is translucent which means that phase separation is not prevented. Indeed, the IPN transparency informs us about phase separation: the more the material is transparent, the more the phase separation is avoided because any light wavelength will be diffracted by any phase domain the size is of the same order of magnitude,

making the material appear translucent to opaque [3]. In the case of a PIB/PMMA 30/70 IPN, the difference between the respective refractive index of both polymers is very weak ($n_{\text{D PMMA}}^{20} = 1.49$ and $n_{\text{D PIB}}^{20} = 1.50$ [36]), which means that if the IPN is not transparent the phase separation is important with domain size at least larger than 100 nm [4].

When the DCPD amount is increased up to 1% by weight with respect to MMA (Fig. 2(c)), both networks form simultaneously during the 80 first minutes at 40°C . The methacrylate function conversion reaches 90% but the PIB network formation is slower than under the previous conditions and the hydroxyl group conversion only reaches 70% after 5 h. The conversion is thus lower than in the previous case, which can be explained by the fact that the synthesis is carried out below the PMMA glass transition temperature. Thus, the PMMA network formation hinders the PIB network formation. This behavior has been already observed during the PMMA/PDMS IPN synthesis in which PMMA network is formed first [17,31]. In order to check this hypothesis, a different initiating system has been chosen for the synthesis of the PMMA network such that it is clearly synthesized before the PIB network. In order to make sure that the PMMA network is completely formed before the PIB one, benzoin methyl ether (3% by weight with respect to MMA) was added as a photosensitizer and the reaction was carried out 2 h at 20°C under UV irradiation. The PIB network is formed as described previously. Then the mixture is heated at 60°C for 2 h in order to synthesize the PIB network. The resulting IPN is white. Thus, when the PMMA network is formed before or at the same time as the PIB network, the final materials are opaque in spite of the weak difference between the refractive indices of both polymers which is characteristic of an important phase separation. Moreover, the amount of extractable material identified as PIB oligomers by ^1H NMR is higher than 12%, indicating that the PIB network formation cannot indeed be completed when the PMMA network is formed first.

Finally, when the IPN synthesis is carried out within the presence of a 0.5% DCPD proportion with respect to PMMA (Fig. 2(b)), the PIB network is formed first, whereas the PMMA network formation starts 1 h later only and is achieved within 30 min. The conversions after 300 min at 40°C are equal to 86 and 100% for PIB and PMMA networks, respectively, and the final material is transparent. Thus a better degree of interpenetration is obtained in this case compared with the two sets of experimental conditions described above. This can be explained by the fact that after 1 h at 40°C the conversion of the PIB network reaches 60%. This PIB network is swollen by MMA and toluene, the PMMA network formation occurs very rapidly and is completed within 30 min. In these conditions the phase separation between PIB and PMMA caused by the lack of compatibility between the two polymers ($\delta_{\text{PIB}} = 18.5 (\text{MPa})^{1/2}$ and $\delta_{\text{PMMA}} = 19.65 (\text{MPa})^{1/2}$ [37]) does not have time to occur. Thus, when the PMMA network is

synthesized soon enough after the PIB network, the interpenetration degree seems to be improved.

Whatever the DCPD proportion it appears that a Trommsdorff effect self-acceleration is observed during the PMMA network formation inducing a slight increase in the hydroxyl conversion rate. This phenomenon is characterized by an increase of the slope of the hydroxyl function conversion curve as a function of time.

In the in situ synthetic pathway which has been chosen for the PIB/PMMA IPNs, PIB and PMMA networks can be formed either simultaneously or sequentially depending on the DCPD amount introduced in the reaction mixture. The best interpenetration degree seems to be obtained when the PIB network is formed first. It is then necessary to ensure that the PMMA network formation occurs as soon as possible in order to avoid or at least minimize the phase separation between both networks. Thus all IPNs the properties of which are discussed below are synthesized with 0.5% DCPD. The reactive mixture is cured at 40 °C for 6 h and post-cured at 80 °C for 1 h. All IPNs are transparent and the extracted materials are lower than 4% in all cases. Analysis of extracted compounds by ^1H NMR shows that they are mainly composed of linear PIB chains of higher molecular weight which are formed by extension reaction through isocyanate functions of the cross-linker.

3.2.2. IPN mechanical and morphological characterizations

An improvement in the poor mechanical properties of PIB was expected in combining PIB and PMMA into an IPN architecture. Thus thermomechanical properties of PIB/PMMA IPNs are studied by DMTA analysis, paying special attention to the influence of IPN composition and cross-linking density.

Fig. 3 shows storage modulus E' and loss factor $\tan \delta$ variations vs. temperature for different IPN compositions ranging from 30 to 80% PMMA by weight, and synthesized according to the conditions described above. All storage modulus are normalized at 3 GPa at -100 °C in order to analyze the modulus evolution as a function of PMMA content.

All IPNs show a dual phase morphology evidenced by two distinct mechanical relaxations at -30 and 140 – 150 °C, corresponding to PIB and PMMA enriched phases, respectively. A partial demixtion between the two components occurs during the synthesis [38].

All samples show a glassy phase below -70 °C. Upon increasing the temperature from -70 to 0 °C, the samples soften and the modulus decreases dramatically. The intermediate plateau value of the elastic modulus is reached at around 0 °C and extends up to around 120 °C which corresponds to the beginning of the PMMA phase mechanical relaxation. The plateau value increases from 0.7 to 200 MPa at 20 °C when PMMA weight proportion increases from 30 to 80%. Thus, the material is more and more rigid on increasing the PMMA content. Above 150 °C, the storage modulus reaches also a plateau the value of

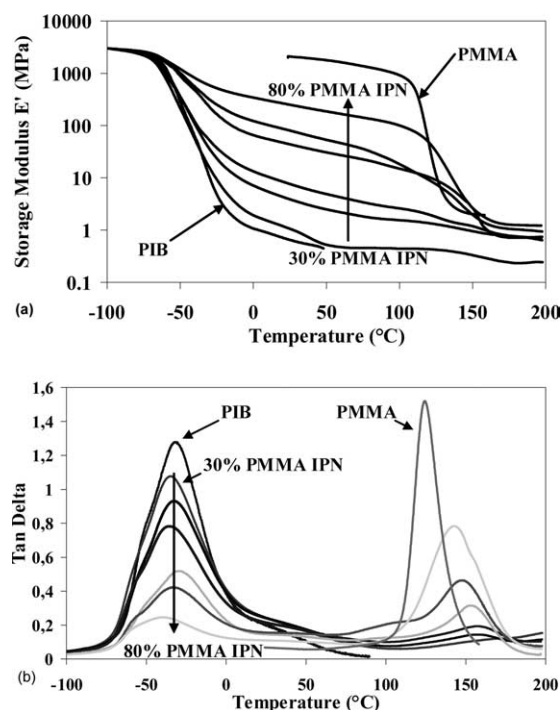


Fig. 3. Thermomechanical properties of PIB/PMMA (80/20, 70/30, 60/40, 50/50, 40/60, 30/70, 10/90) IPNs. (a) storage modulus and (b) $\tan \delta$ vs. temperature. PIB and PMMA single network values are reported.

which increases with PMMA content. Whatever the PMMA weight proportion materials do not flow at higher temperatures and keep a stable modulus value up to 200 °C.

The $\tan \delta$ values are associated with segmental chain motion development and are also greatly influenced by the IPN weight composition. When the PMMA amount decreases the maximum value of $\tan \delta$ peak at -30 °C which corresponds to the mechanical relaxation of the rich PIB phase increases. It reveals interactions that exist between both phases in the IPN. The PIB chain segmental motions are hindered by the PMMA content increase. The same phenomenon has been observed by Brachais et al. [19] in poly(methylphenylsiloxane)(PMPS)/poly(methylmethacrylate) (PMMA) IPN by solid ^1H NMR analysis. The PMPS local chain motions are sensitive to the presence of the PMMA units, which undergoes no chain motion in the studied temperature range. The same phenomenon is believed to arise here. Simultaneously, the maximum value of $\tan \delta$ peak located around 140 °C decreases and changes its shape, thus becoming wider and finally disappearing for the 30% PMMA amount. Moreover, whatever the PMMA proportion this peak which corresponds to the PMMA rich phase, when it is present, is always observed at a temperature which is higher ($T = 158$ °C for PIB/PMMA (50/50) IPN) than that of the PMMA single network ($T = 132$ °C). The same phenomenon has been reported for PDMS/PMMA IPNs and it is explained by a local increase of PMMA phase cross-linking density [14, 39]. In addition to these observations, the $\tan \delta$ shift vs.

temperature has been measured in the case of PIB/PMMA semi-IPNs, i.e. in which the PMMA is uncross-linked (Fig. 4), all synthesis conditions being identical to those of the IPN synthesis except that no EGDM (PMMA cross-linker) is added. The $\tan \delta$ peak of the rich PMMA phase is observed at 152 °C which corresponds to a 20 °C shift compared with the single PMMA network value. The confined PMMA chain environment inside the PIB network might be responsible for this increase of mechanical relaxation temperature.

In order to compare the thermomechanical properties of the same IPN materials at room temperature, storage modulus E' and $\tan \delta$ values at 25 °C are reported in Fig. 5.

When the PMMA content increases from 0 to 50% by weight, IPN storage moduli are weak and increase from 0.75 to 15.5 MPa. The PMMA rich phase has little influence on the material rigidity. Accordingly $\tan \delta$ is nearly constant and equal to 0.20. Thus, these materials show good damping properties and this is in agreement with their flexible macroscopic behavior. In this proportion range (PMMA content below 50%) IPNs behave like vulcanized rubbers the modulus of which increases with a hard filler amount increase. Indeed the Young modulus of a vulcanized rubber is equal to about $E=0.45$ MPa and this value is increased to 0.65 MPa when the material is reinforced [40].

The modulus values measured at 25 °C increase from 90 to 3000 MPa when the PMMA content increases from 60 to 100%. Simultaneously, $\tan \delta$ values decrease linearly from

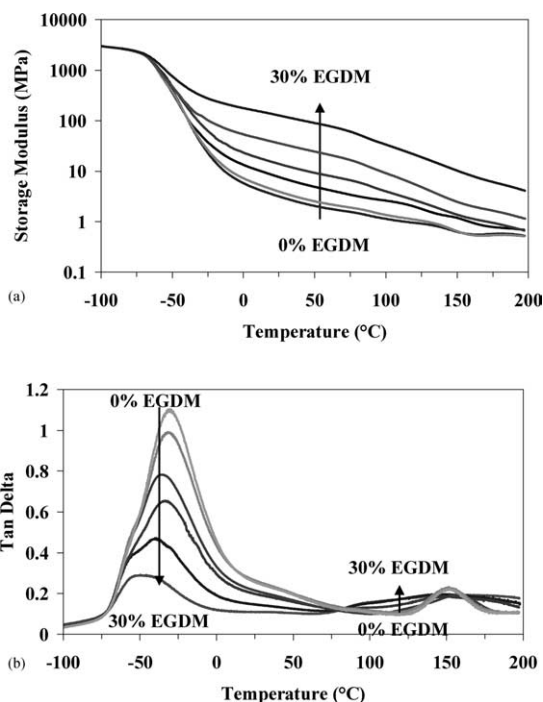


Fig. 4. PIB/PMMA (50/50) IPNs storage modulus (a) and $\tan \delta$ (b) vs. temperature. IPNs are synthesized with different EGDM amounts (0, 1, 3, 10, 20 and 30% by weight with respect to MMA). The arrow indicates EGDM amount increase.

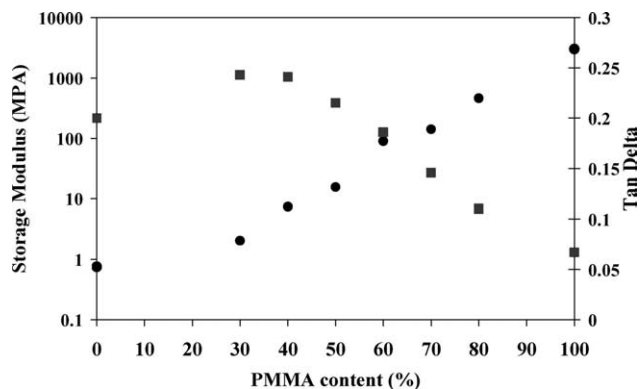


Fig. 5. (●) Storage modulus and (■) $\tan \delta$ measured at 25 °C for PIB/PMMA IPNs with different PMMA contents.

0.20 to 0.07 which corresponds to the PMMA single network $\tan \delta$ value.

Thus, it is possible to improve the PIB network thermomechanical properties by combining it with PMMA into an IPN architecture. The material rigidity depends on the PIB/PMMA relative weight composition. However, a higher rigidity (higher storage modulus) is associated to lesser damping properties (lower $\tan \delta$ values).

Since two mechanical relaxations corresponding to two phases enriched in one of the two polymers (PIB and PMMA rich phases, respectively) are detected by DMTA, it can be concluded that the IPNs described here show a phase separation. However, the phase separation extent might be reduced if the cross-linking density of at least one of the two networks is increased [12,16]. For this reason, the PMMA cross-linking density effect on the IPN thermomechanical properties has been studied on IPNs with various PIB/PMMA weight proportions. Except for the EGDM amount which controls the cross-linking density of the PMMA network, the other network synthesis conditions are kept identical.

In a first step, PIB/PMMA (70/30) IPNs in which PIB is the main component, have been synthesized with different EGDM weight proportions with respect to MMA (from 0 to 30%) and further characterized by DMTA. The storage moduli and PIB $\tan \delta$ peak of this series of IPNs are slightly affected by the PMMA cross-linking density compared with the storage modulus measured previously (3% EGDM by weight with respect to MMA).

The PMMA cross-linking density increase mainly acts on the PMMA rich phase. Although the PMMA mechanical relaxation is undetectable for this weight proportion it might indirectly be reflected on the behavior of the PIB rich phase. Thus PMMA is present in the PIB rich phase but does not form a continuous phase over the whole material considering the low modulus values measured at temperatures higher than that of PIB mechanical relaxation. Those observations are in agreement with the macroscopic aspect of the IPNs which behave as reinforced rubbers.

In a second step, the thermomechanical properties of

PIB/PMMA (50/50) IPNs in which the EGDM amount varies from 0 to 30% by weight with respect to MMA are shown in Fig. 4. The two mechanical relaxations are always present whatever the PMMA cross-linking density used. Thus the increase in the cross-linker proportion does not allow a complete suppression of phase separation but affects the PIB/PMMA (50/50) IPN thermomechanical properties. Both the intermediate plateau position and the storage modulus values after PMMA mechanical relaxation temperature increase with the cross-linking density. For example the storage modulus plateau value of the IPN containing 30% EGDM is 40 times higher than that of the semi-IPN (without EGDM, i.e. with no cross-link at all). Thus the increase in PMMA cross-linking density indeed affects both the PMMA rich phase and the whole material properties.

The PMMA cross-linking density has also an important influence on the $\tan \delta$ curves. When the EGDM amount increases from 10 to 30% the height of $\tan \delta$ peak at -30°C corresponding to PIB mechanical relaxation decreases. The PIB chain segmental motions are also hindered by the PMMA cross-linking density increase [19]. Simultaneously, the PMMA rich phase mechanical relaxation peak becomes broader, its height decreases and it is shifted towards lower temperatures. This shift shows that a lower energy amount is required to promote PMMA chain segmental motions, which are probably plasticized by PIB phase. This is characteristic of improved phase interpenetration. Thus the PMMA network cross-linking density increase improves the network interpenetration if the EGDM content is higher than 10% by weight with respect to MMA.

Those results also bring information about the respective phase organization. Indeed, the PMMA network cross-linking density increase induces a higher rigidity both in the PMMA rich phase and in the whole materials because the IPN modulus values before the PMMA mechanical relaxation increase also. This is possible only if the PMMA dispersed phase is locally interconnected.

Finally, the PMMA cross-linking density effect on PIB/PMMA (30/70) IPN thermomechanical properties has been examined, i.e. where PMMA is the major component. The cross-linking density effect on this IPN is identical to what is observed on PIB/PMMA (50/50) IPN i.e. the phase interpenetration extent is improved by a PMMA network cross-linking density increase and local PMMA dispersed phase interconnection is evidenced.

This thermomechanical properties study has shown that PIB/PMMA (70/30) IPNs behave like PMMA reinforced rubbers. When the PMMA weight proportion increases in the materials (50/50 and 30/70 compositions) PMMA dispersed domains are locally interconnected and the whole material becomes more rigid. However, the increase in PMMA cross-linking density does not allow obtaining a close to homogeneous phase with a unique mechanical relaxation situated at a temperature in between those of single networks by DMTA.

The DMTA analysis enlightens some characteristics of the IPN morphology which have been confirmed by AFM measurements. AFM analyses in tapping mode were performed on two PIB/PMMA IPN surfaces with different PMMA weight proportions. The image contrast is given by the stiffness difference between PIB and PMMA rich phases. Thus the PIB rich phase appears dark and the PMMA rich phase appears clear on the image. The images of a PIB rich IPN (PIB/PMMA (60/40)) surface are reported Fig. 6. The PIB rich phase represents the continuous phase (matrix) in which rich PMMA nodules are dispersed (clear phase). The nodule size is about 50 nm which is in agreement with the phase domain sizes generally reported for the IPN materials [41]. Those nodules exhibit various shapes whatever the observation scale. Thus the conclusions which can be drawn from those images are in agreement with the morphology suggested by the thermomechanical properties analysis although the surface morphological characteristics are known to be often different from the bulk ones [42,43]. However, because of the very tight entanglement between polymer chains, which results from the IPN architecture in this particular case, the surface organization might reflect the bulk structure more than expected for linear polymers, single polymer networks and co-networks. It would especially be the case in PMMA/PIB IPNs, where at room temperature the material is below the glass transition of the ‘hard’ polymer partner in the IPN which will hinder the motions of the ‘soft’ component. Indeed AFM and TEM images of polystyrene/PIB IPNs (to be published) show a close to identical morphology both at the surface and in the bulk.

A PMMA enriched (PIB/PMMA (30/70) IPN) has been also examined by AFM analysis (Fig. 7). Although not being the predominant component, the PIB partner still plays the role of the matrix. Indeed, the PIB rich phase (in dark) can be identified as the continuous one over the whole material whatever the observation scale. The PMMA rich phase appears as dispersed domains with various shapes, which seem to result from PMMA nodule interconnection. Thus as evidenced at the surface level by AFM this IPN also presents the morphology predicted from DMTA measurements, corresponding to bulk partially interconnected PMMA domains into a PIB matrix.

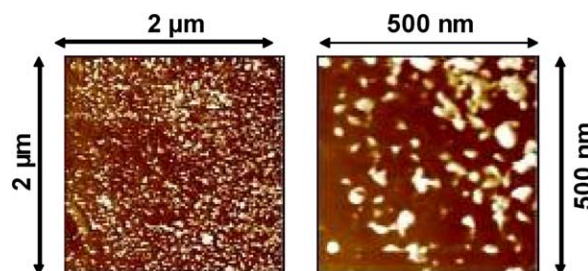


Fig. 6. AFM images of PIB/PMMA (60/40) IPN.

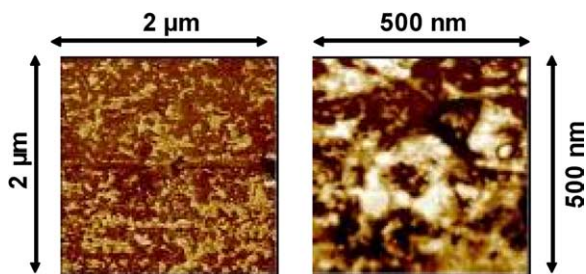


Fig. 7. AFM images of PIB/PMMA (30/70) IPN.

4. Conclusion

To our knowledge, this paper reports the first association of a PIB network with a thermoplastic network into an interpenetrating polymer network (IPN) architecture. Thus PIB/PMMA IPNs in which PIB and PMMA networks are independently cross-linked have been synthesized and characterized. The highest interpenetration degree is obtained when IPNs are synthesized through a in situ synthesis in which the PIB network is formed prior to the PMMA one. The resulting IPNs are transparent but they show two distinct mechanical relaxations at about -70 and $+140$ °C corresponding to rich PIB and rich PMMA phases for all studied compositions and PMMA cross-linking densities. In all cases, the mechanical properties of the PIB network are tremendously improved by the introduction of the PMMA network in the IPN architecture, which was the aim of this work. The bulk mechanical properties of the IPNs change as a function of the PMMA content and can be correlated to their surface morphology observed by AFM analysis.

Acknowledgements

The authors thank BASF for its financial support, and particularly Dr H-P. Rath who supported this research and provided the α,ω -dihydroxy polyisobutene samples. They thank Dr R. Blackborow for many stimulating discussions, Drs F. Vidal and B. Amana for assistance in carrying out the DMTA analysis and AFM measurements, respectively.

References

- [1] Othmer K. Encyclopedia of chemical technology. New York: Wiley; 1998.
- [2] Teysssié D, Vancaeyzeele C, Laskar J, Fichet O, Boileau S, Blackborow R, et al. Molding compound. Patent number WO2005019285; 2005.
- [3] Sperling LH, Mishra V. IPNs around the world: science and engineering. New York: Wiley; 1997. p. 1–25.
- [4] Sperling LH. Interpenetrating polymer networks. In: Sperling LH, Klemmner D, Utracki LA, editors. Advances in chemistry series, vol. 239. Washington, DC: American Chemical Society; 1994. p. 3–38.
- [5] Sherman MA, Kennedy JP, Ely DL, Smith D. J Biomater Sci Polym 1999;10(3):259–69.
- [6] Sherman MA, Kennedy JP. J Polym Sci Part A 1998;36:1901–10.
- [7] Sherman MA, Kennedy JP. J Polym Sci: Part A 1998;36:1891–9.
- [8] Ivan B, Almdal K, Mortensen K, Johannsen I, Kops J. Macromolecules 2001;34(6):1579–85.
- [9] Erdodi G, Ivan B. Chem Mater 2004;16(6):959–62.
- [10] Janecska A, Ivan B. Polym Mater Sci Eng 1998;79:477–8.
- [11] Jia DM, You CJ, Wu B, Wang MZ. Int Polym Process 1988;3(4): 205–10.
- [12] Wang SH, Zawadzki S, Akcelrud L. J Polym Sci Part B: Polym Phys 2000;38(22):2861–72.
- [13] He XW, Widmaier JM, Herz JE, Meyer GC. In: Klemmner D, Frisch KC, editors. Advance interpenetrating polymer networks, Lancaster, Technomic, 1994. p. 321–56.
- [14] He XW, Widmaier JM, Herz JE, Meyer GC. Polymer 1992;33(4): 866–71.
- [15] He XW, Widmaier JM, Herz JE, Meyer GC. Polymer 1989;30(2): 364–8.
- [16] Zhou P, Frisch HL, Rogovina L, Makarova L, Zhdanov A, Sergeienko N. J Polym Sci Part A: Polym Chem 1993;31(10): 2481–91.
- [17] Zhou P, Xu Q, Frisch HL. Macromolecules 1994;27(4):938–46.
- [18] Frisch HL, Xu Q, Zhou P. Polym Gels Networks 1994;2(3/4):257–66.
- [19] Brachais L, Lauprêtre F, Caille JR, Teyssié D, Boileau S. Polymer 2002;43(6):1829–34.
- [20] Kennedy JP, Askew MJ, Richard GC. J Biomater Sci 1993;4:445–9.
- [21] Nia H, Aaserudb DJ, Simonsick Jr WJ, Souceka MD. Polymer 2000; 41:57–71.
- [22] Stansbury JW, Dickens SH. Dent Mater 2001;17:71–9.
- [23] Schapman F, Couvercelle JP, Bunel C. Polymer 1998;39:965–71.
- [24] Fichet O, Vidal F, Laskar J, Teyssié D. Polymer 2005;46:37–47.
- [25] Puskas JE, Antony P, El Fray M, Altstädt V. Eur Polym J 2003;39(10): 2041–9.
- [26] Storey RF, Baugh DW. Polymer 2001;42(6):2321–30.
- [27] Plazek DJ, Chay IC, Ngai KL, Roland CM. Macromolecules 1995; 28(19):6432–6.
- [28] Ngai KL, Plazek DJ. Macromolecules 2002;35(24):9136–41.
- [29] Frick B, Richter D. Phys Rev B 1993;47(22):14795–804.
- [30] Widmaier JM, Drillières S. J Appl Polym Sci 1997;63(7):951–8.
- [31] Zhou P, Frisch HL. Macromolecules 1994;27(7):1788–94.
- [32] Schapman F, Couvercelle JP, Bunel C. Polymer 1998;39(4):965–71.
- [33] Laskar J, Vidal F, Fichet O, Gauthier C, Teyssié D. Polymer 2004; 45(15):5047.
- [34] Brandrup J, Immergut EH, Grulke EA. Polymer handbook. 4th ed. New York: Wiley; 1999.
- [35] Odian G. Principle of polymerization. 3rd ed. New York: Wiley; 1991.
- [36] Seferis JC. In: Brandrup J, Immergut EH, Grulke EA, editors. Polymer handbook. New York: Wiley; 1999. Chapter 4.
- [37] Ruzette AVG, Mayes AM. Macromolecules 2001;34(6):1894–907.
- [38] Sophiea D, Klemmner D, Sendjarevic V, Suthar B, Frisch KC. Interpenetrating polymer networks. In: Sperling LH, Klemmner D, Utracki LA, editors. Advances in chemistry series, vol. 239. Washington, DC: American Chemical Society; 1991. p. 39–76.
- [39] Tabka MJ, Widmaier JM, Meyer JC. Sound and vibration damping with polymers. Washington, DC: ACS; 1990.
- [40] Billmeyer FW. Textbook of polymer science. 3rd ed.: Wiley; 1984.
- [41] Qin CL, Cai WM, Cai J, Tang D-Y, Zhang JS, Qin M. Mater Chem Phys 2004;85(2/3):402–9.
- [42] Bruns N, Scherble J, Hartmann L, Thomann R, Ivan B, Mülhaupt R, et al. Macromolecules 2005;38:2431–8.
- [43] Yoon SC, Ratner BD, Ivan B, Kennedy JP. Macromolecules 1994;27: 1548–54.